ceramics

MDPI

Article

The Effect of Adding Banana Fibers on the Physical and Mechanical Properties of Mortar for Paving Block Applications

Ginan Al-Massri [1], Hassan Ghanem [1,*], Jamal Khatib [1,2,*], Samer El-Zahab [3] and Adel Elkordi [1,4]

[1] Faculty of Engineering, Beirut Arab University, Beirut 12-5020, Lebanon; g.massri@bau.edu.lb (G.A.-M.); a.elkordi@bau.edu.lb (A.E.)
[2] Faculty of Engineering, University of Wolverhampton, Wolverhampton WV1 1LY, UK
[3] College of Engineering and Technology, American University of the Middle East, Egaila 54200, Kuwait; samer.el-zahab@aum.edu.kw
[4] Faculty of Engineering, Alexandria University, Alexandria 5423021, Egypt
* Correspondence: h.ghanem@bau.edu.lb (H.G.); j.khatib@bau.edu.lb (J.K.)

Abstract: Paving blocks might encounter diverse environmental conditions during their lifespan. The durability of paving blocks is determined by their capacity to endure various exposure conditions. Synthetic fibers have been used in mortar and concrete to improve their properties. This research investigates the influence of including banana fiber (BF) on the physical and mechanical characteristics of mortar. Five different mortar mixes were developed, with varying amounts of BF ranging from 0 to 2% by volume. Testing included ultrasonic pulse velocity, compressive strength, flexural strength, total water absorption, and sorptivity. Specimens were cured for up to 90 days. The results indicate that using 0.5% BF resulted in an improvement in compressive and flexural strength compared to the control mix. There was an increase in total water absorption and the water absorption coefficient in the presence of fibers. There appeared to be good correlations between the compressive strength and the other properties examined.

Keywords: natural fibers; bio-fibers; mortar; strength; total water absorption; capillary water absorption

Citation: Al-Massri, G.; Ghanem, H.; Khatib, J.; El-Zahab, S.; Elkordi, A. The Effect of Adding Banana Fibers on the Physical and Mechanical Properties of Mortar for Paving Block Applications. *Ceramics* **2024**, *7*, 1533–1553. https://doi.org/10.3390/ceramics7040099

Academic Editors: Francesco Baino, Pardeep Gianchandani, Enrico Fabrizio, Bartolomeo Megna and Manuela Ceraulo

Received: 28 August 2024
Revised: 11 October 2024
Accepted: 14 October 2024
Published: 23 October 2024

1. Introduction

The world's agricultural sector generates almost one billion tons of waste per year. Plant byproducts account for 80% of these pollutants [1]. Ecologists are concerned about these pollutants because of their negative impact on underground water sources and the ozone layer, two factors that strongly affect global warming and economic conditions [2]. Thus, part of these wastes was incorporated into cementitious-based materials used in building and paving construction. Natural fibers derived from plants are recognized as eco-friendly alternatives to synthetic fibers because of their abundance, affordability, longevity, and minimal energy consumption [3,4].

The mechanical properties of natural fibers are influenced by their chemical structure. As a result, the engineering features of cement matrices reinforced with natural fibers are improved to a level that is comparable to those of cement matrices reinforced with synthetic fibers [5]. The mechanical properties of concrete and mortar were investigated in previous studies addressing the effect of adding natural fibers to the mixture in terms of the total volume or total mass. For instance, Shah et al. [6] investigated the effect of varying the mass fractions of coconut and sisal fibers in high-strength concrete (HSC) from 0.5 to 1.5% of the cement content on the material's characteristics. At a fiber concentration of 1%, HSC's compressive strength was increased by 33% with coconut fibers and 24% with sisal fibers. According to Khan et al. [7], jute fiber boosts the mechanical properties of concrete, including its compressive strength, split tensile strength, and flexural strength. It was found that a ratio of 0.10% jute fiber is optimum for enhancing these features. The

addition of coir fiber to concrete up to 0.5% by mass of mixture increased the material's strength, as reported by Prafulla et al. [8].

Regarding permeability, the addition of treated natural fibers to cement-based matrices can significantly reduce their total water absorption, contributing to the sustainability and durability of the material. As an illustration, Machaka et al. [9] reported that adding up to 1.5% of Phragmites Australis (PA) natural fibers to concrete can decrease water absorption by total immersion and capillary action by up to 45%, with a negligible decrease in concrete density and strength. This suggests that natural fibers can enhance the durability of concrete by reducing its susceptibility to water ingress [9]. Zouaoui et al. [10] showed that natural fibers such as palm stem and hemp fibers, when treated to reduce their hydrophilic nature, can be integrated into mortar to produce materials with low thermal conductivity and an excellent moisture-buffering capacity. Contradictorily, untreated natural fibers may absorb water due to their hydrophilic nature, which can be a challenge for their use in concrete. Li et al. [11] discussed the hydrophilic behavior of natural fibers, which can lead to reduced bonding between the concrete matrix and fibers, potentially affecting the overall performance of the concrete material. However, the chemical alteration of natural fibers demonstrates significant potential for enhancing their mechanical properties, boosting dimensional stability against moisture and biodeterioration, hence prolonging service life and expanding applicability. A multitude of reviews exists regarding the chemical modification of fibers using various substances. There are numerous approaches aimed at efficiently modifying the fiber's surface to render it hydrophobic. Alkaline treatment, acylation, and silylation represent the predominant chemical treatments [12,13]. Therefore, the use of treated natural fibers in concrete is a promising strategy for producing eco-friendly building materials with adequate mechanical and durability performance [9].

Worldwide, banana harvesting produces thousands of tons of agricultural waste [14]. Previous research showed that, up to a certain point, cementitious materials' mechanical characteristics can be improved by adding banana fiber (BF). As an example, Babar Ali et al. [15] investigated the impact of varying amounts of banana stem fiber BSF (0.25, 0.5, and 1% of the total mix volume) on the strength characteristics of concrete. The results showed that the compressive strength, splitting tensile strength, and flexural strength of the concrete were enhanced by 6, 40, and 10%, respectively, when incorporating BSF at 0.5% content. Logeshwar et al. [16] investigated the performance of composites made from concrete mixed with agricultural waste (bagasse ash (BA) and rice husk ash (RHA)) at different percentages of BF (0.2, 0.4, and 0.6%). Incorporating BF into concrete mixes with BA and RHA significantly enhanced their strength. When comparing several BF combinations, the one with 0.2% BF yielded the best results. Pathan et al. [17] examined the compressive and flexural strengths of high-strength concrete by varying the amount of BF from 0 to 2% of the weight of cement and observed that the mix of 1.5% BF generated the strongest results. The impact of different concentrations of BF of a 10 mm length on the mechanical properties of mortar was investigated by Lamichhane et al. [18]. Adding 0.25% BF to base mortar increased compressive strength by 18.7%, flexural strength by 29.9%, and splitting tensile strength by 41.1% after 28 days.

In terms of physical properties, the available sources do not explicitly quantify the specific effect of BF on the ultrasonic pulse velocity and total and capillary water absorption of mortar. To obtain a final verdict on this matter, additional research and experimental evidence are necessary. Considering the paucity of literature on the subject, this research sets out to fill that gap by investigating the physical and mechanical characteristics of mortar containing BF. In light of this, a sequence of experiments was carried out on mortar samples with different BF additions by total volume (0, 0.5, 1, 1.5, and 2%). Tests covered ultrasonic pulse velocity (UPV), compressive strength, flexural strength, total water absorption (TWA), and capillary water absorption (CWA). The experimental data in this study were thoroughly validated using a hyperbolic model to predict compressive strength and a capillary-diffusive model to estimate diffusion and sorptivity coefficients. These models were selected for their capacity to provide an extensive and comprehensive depiction of

the underlying physical properties of the material under varying environmental conditions. This approach's innovation resides in the integration of these two models, which not only provides a more accurate prediction of mechanical properties and moisture-transport characteristics but also addresses traditional empirical approaches with advanced, physics-based simulations. This novel integration promotes a more profound comprehension of the relationship between material strength and moisture dynamics, providing insights that can substantially improve the design and efficacy of materials in practical applications. Furthermore, the correlations among several characteristics are examined in this study.

2. Materials and Methods

2.1. Materials

BF was harvested from banana pseudo-stems by means of a decortication machine in Cairo, Egypt. After slicing the BF into 1 cm pieces, it was immersed in a 6% NaOH solution for 24 h [19]. Next, BF was rinsed with clean water to neutralize the alkali, and lastly, it was sun-dried. Having been cleaned, dried, and then packed in plastic bags, the fibers were ready for use. Figure 1 represents the raw and cut-treated BF. The process of obtaining BF is shown in Figure 2. The bulk density of BF is 1350 kg/m^3. The stress–strain curve for BF is displayed in Figure 3. The curve shows the relationship between the applied stress and the resulting strain, revealing that the fibers can withstand increasing loads without breaking. The tensile strength is 53 MPa, and the elastic modulus is 3.5 GPa.

(**a**) (**b**)

Figure 1. (**a**) Raw bundled BF, (**b**) Cut-treated BF.

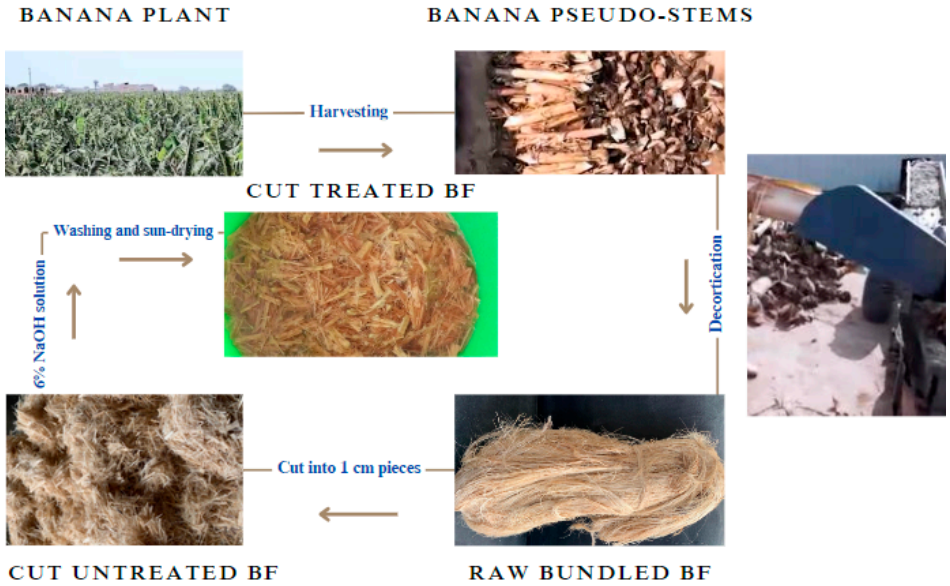

Figure 2. Preparation process of banana fiber.

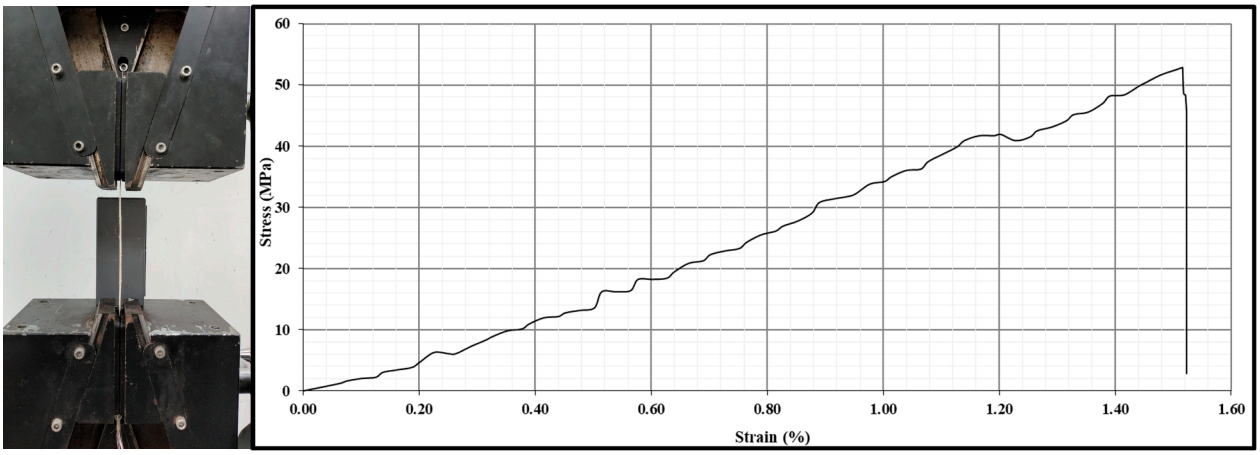

(**a**) (**b**)

Figure 3. (**a**) BF tensile strength test; (**b**) Stress–strain curve.

Type I Ordinary Portland Cement with 3.15 specific gravity and 1440 kg/m^3 density was employed. Siliceous sand with 2.8 fineness modulus, 3.5% water absorption, and specific gravity of 2.65 was used.

2.2. Mix Proportions

Five distinct percentages (0, 0.5, 1, 1.5, and 2% by volume) of BF were incorporated into the mortar mixes. For all mixes, the cement-to-water -to-sand (c:w:s) ratio remained constant at 1:0.45:2. Mix proportions are displayed in Table 1.

Table 1. Mortar mix proportions.

	Quantity (kg/m^3)						
Mortar Code	**Cement**	**Water**	**Sand**	**BF**	**BF (% by vol)**	**w/c**	**c/s**
M-0% BF	657	295.6	1314	0	0	0.45	0.5
M-0.5% BF	657	295.6	1314	6.75	0.5	0.45	0.5
M-1% BF	657	295.6	1314	13.5	1	0.45	0.5
M-1.5% BF	657	295.6	1314	20.25	1.5	0.45	0.5
M-2% BF	657	295.6	1314	27	2	0.45	0.5

2.3. Experimental Methodology

2.3.1. Mortar Sample Preparation

Initially, a dry mixture of cement, sand, and BF was prepared. Subsequently, water was introduced and agitated for a duration of two minutes. Following the mixing process, the mortar's consistency was assessed by conducting the flow test according to ASTM C 1437 [20]. The flows corresponding to M-0% BF, M-0.5% BF, M-1% BF, M-1.5% BF, and M-2% BF were 103, 96, 89, 81, and 77%, respectively. Flow table values exhibited a negative correlation with increasing BF%, as observed from the flow findings. Ultrasonic-pulse velocity and compressive strength tests were conducted on cubes with dimensions of 50 × 50 × 50 mm. Beams measuring 40 × 40 × 160 mm were used to determine flexural strength. For total water absorption and capillary water absorption, cubes measuring 100 × 100 × 100 mm were utilized.

2.3.2. Ultrasonic-Pulse Velocity (UPV)

One nondestructive method for evaluating concrete quality is UPV test. This method involves tracking the speed of an ultrasonic pulse wave as it travels through the concrete sample. The method is standardized by ASTM C597 [21]. UPV test was conducted at

1, 7, 28, and 90 days (Figure 4). Concrete quality is classified according to pulse velocity values, as presented in Table 2.

Figure 4. UPV test.

Table 2. Concrete quality classification based on UPV. Reproduced with permission from [22], Digital Commons @ BAU, 2024.

Quality of Concrete	Excellent	Good	Doubtful	Poor	Very poor
UPV (km/s)	>4.5	3.5-4.5	3.0-3.5	2.0-3.0	<2.0

2.3.3. Compressive Strength

The compressive strength test, considered as an indicator of the quality of the mortar, is affected by various parameters, including mix quantities, water-to-cement ratio, and curing methods. The ASTM C109 [23] was followed to measure the compressive strength at 1, 7, 28, and 90 days (Figure 5). The compressive strength value was taken as the average of three readings.

Figure 5. Compressive strength test.

2.3.4. Compressive Strength Modeling

Two variables, the initial rate of compressive strength (IRC) and the ultimate compressive strength (UC), are used to calculate compressive strength characteristics. As a measure of the material's early strength gain from moisture, the IRC indicates the rate of compressive strength during the initial phases of curing. On the other hand, the ultimate compressive strength (UC) defines the highest level of compressive strength, describing the long-term behavior of the material after reaching a constant moisture content. In order to examine these key variables, a hyperbolic model [24] (Figure 6) was generated as follows:

$$C = \frac{x}{\frac{1}{y} + \frac{x}{z}} \quad (1)$$

where the following apply:
C = modeled compressive strength;
x = curing period (days);
y = initial rate of compressive strength (IRC);
z = ultimate compressive strength (UC).

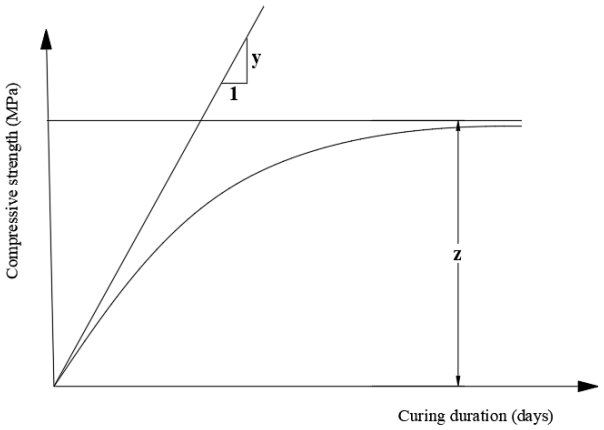

Figure 6. Compressive strength variables.

The aforementioned two variables were determined using the solver built in Microsoft Excel software version 2021.

2.3.5. Flexural Strength

The flexural strength test is an indirect test employed to quantify the tensile strength of mortar samples at days 1, 7, 28, and 90 following ASTM C348 [25] (Figure 7). The flexural strength value was the average of three samples.

Figure 7. Flexural strength test.

2.3.6. Total Water Absorption (TWA)

Mortar samples were subjected to TWA test measuring the amount of water absorbed after a particular duration according to ASTM C1585 [26] (Figure 8). After 1, 7, 28, and 90 days of curing, the mortar specimens were dried at 80 °C for 48 h until they reached a constant dry weight (A). The cubes were then submerged in water for 5 min, taken out, dried using a towel to remove surface water, and weighed again; at this point, the weight was recorded as the initial weight (B). At 10, 20, 60, 120, and 450 min intervals, this process was repeated. The percentage of TWA was calculated as follows:

$$TWA = \frac{B - A}{A} \times 100 \quad (2)$$

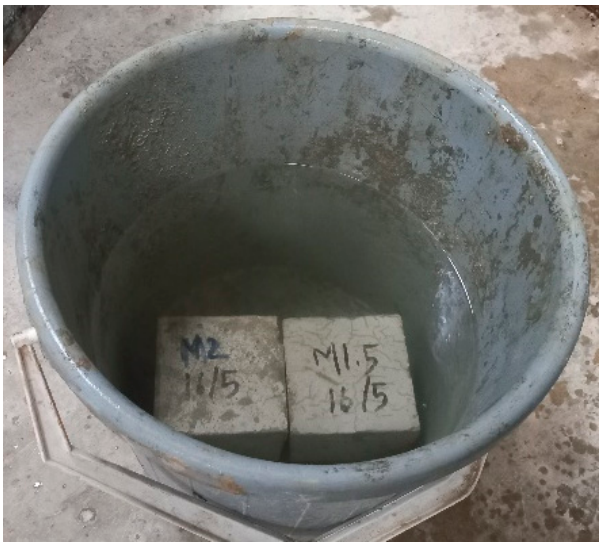

Figure 8. Total water absorption test.

2.3.7. Capillary Water Absorption (CWA)

After being dried at 80 °C until the sample reached a constant mass, mortar specimens were subjected to CWA test following ASTMC1585 [26]. To prevent the evaporation of water and to keep the uniaxial water flow constant during the test, a non-absorbent coating was applied to all four sides of the cubes. Both the top and bottom sides remained unsealed, and the weight of the sample was noted, W_1. As illustrated in Figure 9, the specimen was subsequently placed in a container and filled with water until it reached a depth of 5 mm, as measured from the bottom of the mortar cubes. Measurements of water absorption were taken at 3, 5, 10, 20, 30, 60, 120, and 240 min and 1, 2, and 3 days. The CWA was calculated as follows:

$$CWA = \frac{w_2 - w_1}{A \times d} \quad (3)$$

where the following apply:
$w_2 - w_1$ = cumulative water absorption (g);
A = surface area of the cube through which water penetrates (mm^2);
d = density of water (g/mm^3).

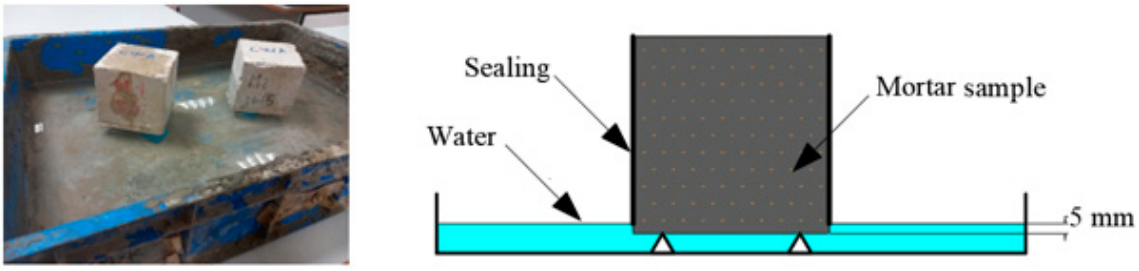

(**a**) (**b**)

Figure 9. (**a**) CWA samples; (**b**) Experiment set-up.

2.3.8. Capillary-Diffusive Model

Water transport in mortar and concrete has been the subject of extensive research. During the first absorption period, the cumulative water absorption M/A is directly proportional to the square root of the elapsed wetting time t, when mortar or concrete surface is exposed to wetting by water. Once water has passed through all of the larger capillary pores, the initial rate of ingress shown reduces after a period of sorption. As time progresses, the significance of small pores grows, suggesting that sorptivity is now happening through the finer pores. As a result of gravitational forces, the rate of sorption is expected to decrease exponentially [27,28]. The transition from rapid to slow sorption rates is modeled using the following capillary-diffusive model [28]:

$$\frac{M}{A} = C\rho\left[1 - \exp\left[\frac{-s\sqrt{t}}{C\rho}\right]\right] + C_O L\left[1 - \frac{8}{\pi^2}\sum_{n=0}^{\infty}\frac{1}{(2n+1)^2}\exp\left[-\frac{(2n+1)^2\pi^2}{4L^2}Dt\right]\right] \quad (4)$$

where the following apply:
M/A = weight of water absorbed per unit of area (kg/m^2);
C = constant associated with the distance from the concrete surface where capillary pores regulate the initial sorption;
ρ = density of the water (kg/m^3);
S = sorptivity coefficient (kg/m^2.s$^{1/2}$);
t = time (s);
C_O = invariance of water concentration (kg/m^2);
L = depth of the sample = 0.1 m;
D = diffusion coefficient (m^2/s).

The aforementioned variables were calculated using the solver built in Microsoft Excel software.

3. Results and Discussion

3.1. Ultrasonic-Pulse Velocity (UPV)

The UPV results for the mortar mixes are shown in Figure 10. A minor reduction in the UPV was observed at all curing ages when 0.5, 1, 1.5, and 2% BF were integrated. As an illustration, the UPV at 90 days for the control mix was 3.88 Km/s. With the addition of 0.5, 1, 1.5, and 2% BF, the associated UPV values were 3.83, 3.71, 3.65, and 3.63 Km/s. The corresponding decreases in the UPV were 1.3, 4.38, 6, and 6.44%. This slight decrease may be due to the fact that fibers have the potential to generate heterogeneity and voids in the mortar's matrix. BF, like other organic fibers, alters matrix homogeneity, which may reduce internal structure continuity. This disturbance may impede ultrasonic pulse transmission, reducing the UPV. Fibers can cause local microstructure abnormalities such fiber-matrix bonding or fiber dispersion, reducing composite material density and homogeneity. These factors can slow ultrasonic waves, which are sensitive to material structural changes. The effects of increasing fiber volume on concrete homogenization and UPV have been

demonstrated in earlier research using different organic fibers, such as coir fiber [29], cotton fiber, and wool fiber [30]. For example, using banana fibers in concrete reduced the UPV by 7% at a 1% fiber volume [15].

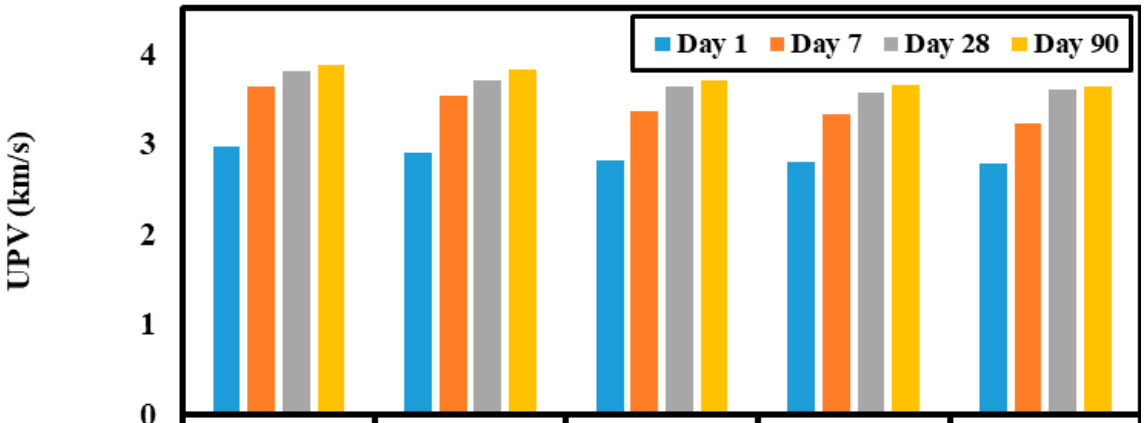

%BF	M-0% BF	M-0.5% BF	M-1% BF	M-1.5% BF	M-2% BF
Day 1	2.97	2.9	2.82	2.8	2.78
Day 7	3.64	3.54	3.36	3.32	3.23
Day 28	3.8	3.7	3.64	3.57	3.6
Day 90	3.88	3.83	3.71	3.65	3.63

Figure 10. UPV of mortar with different BF additions.

3.2. Compressive Strength

The compressive strength of several mortar mixes containing BF is presented in Figure 11. At 90 days, the results demonstrate that adding 0.5% BF resulted in a 7% improvement in compressive strength when compared to the control mix. A potential explanation is that the 1 cm fibers, when introduced to the matrix at a dosage of 0.5%, are distributed uniformly. The increased compressive strength as compared to plain mortar may be due to two factors: the alveolar structures on the surface of the fibers, which form the bond between the mortar and the fibers, and the tensile strength of the BF [31–33]. When compared to the control mix, the compressive strength is 20% lower for M-1% BF, 25% lower for M-1.5% BF, and 47% lower for M-2% BF. The primary chemical ingredient of BF, cellulose, may be responsible for this decrease. Cellulose, owing to its hydrophilic properties, can disrupt the cement-hydration process by competing for water, which is required for the hydration processes necessary for cement setting and strength development. The competition for water can diminish the quantity available for calcium silicate hydrate (C-S-H) gel formation, obstructing the hydration process and potentially compromising the mechanical qualities of the cement. Moreover, the contact between cellulose fibers and the cement matrix may result in the breaking of hydrogen bonds at the fiber–matrix interface, especially as water is absorbed during the curing process. This rupture weakens the bond between the fibers and the matrix, resulting in a decrease in the material's overall strength [34–37]. In line with this pattern is the finding of Lakawa [38], who demonstrated a 7.3% increase in compressive strength when cementitious materials were supplemented with palm fibers at dosages up to 0.5%.

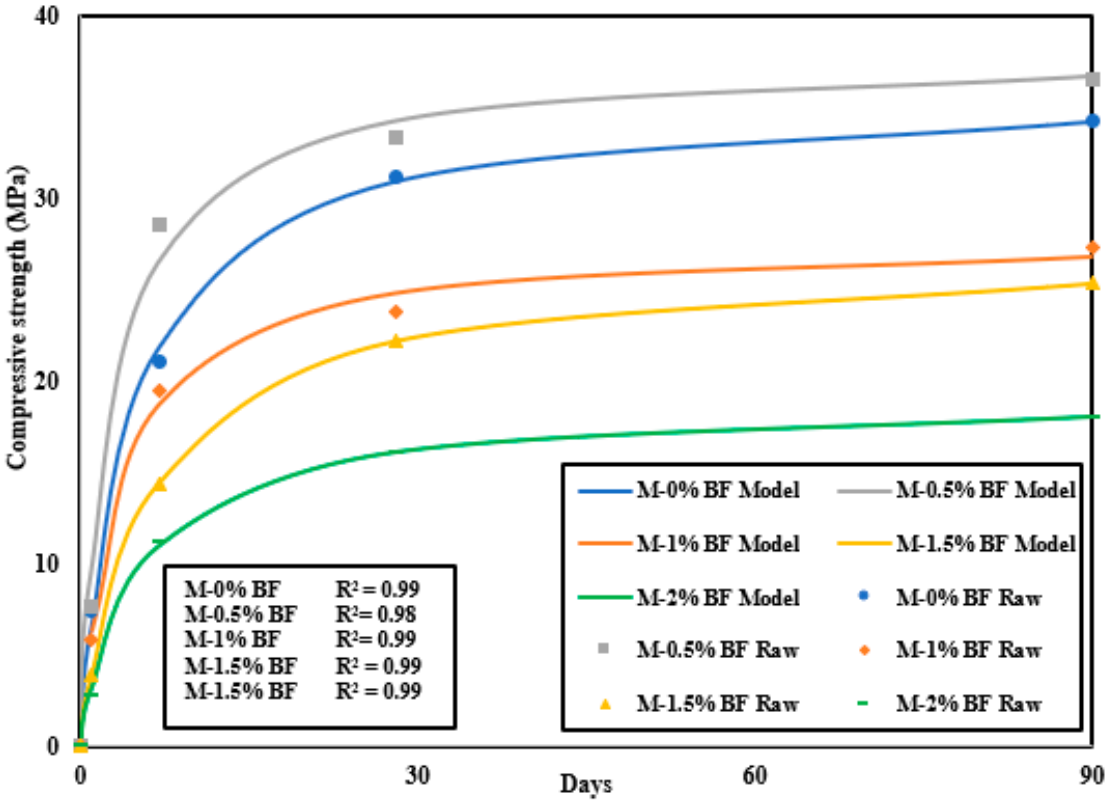

Figure 11. Modeling of the compressive strength of mortar with different BF additions.

A hyperbolic equation that attempted to simulate the mortars' compressive strength with time revealed promising outcomes, showing a significant agreement with the experimental results. R^2 values of 0.99, 0.98, 0.99, 0.99, and 0.99 for 0%, 0.5%, 1%, and 2% BF additions, respectively, indicated a high level of determination. The IRC and UC values for all mortar mixes are displayed in Figure 12. It is evident that these two variables followed an identical pattern. The mortar with 0.5% BF showed an increase in IRC and UC compared to the control mix by 53 and 6%, respectively. The increased values of IRC and UC observed for M-0.5% BF can be attributed to the presence of 0.5% BF, which promotes a uniform dispersion of fibers throughout the mortar matrix, resulting in a strong bonding structure. The regular distribution of fibers throughout the matrix enhances the efficiency of the hydration process during the initial curing stages, generating more consistent hydration rates. This consistency enhances microstructural development, leading to improved ultimate compressive strength of the composite material once a steady moisture content is attained. IRC experienced a gradual decrease of 4, 46, and 55% with 1, 1.5, and 2% BF, respectively, compared to the control mix. The decrease in the initial rate of strength can be related to the chemical consistency of cellulose, which hinders the hydration process of cement [31,34]. Similarly, UC values dropped progressively by 23, 25, and 47% in comparison to the control mix with the addition of 1, 1.5, and 2% BF. The drop in the ultimate strength may be due to the disruption of hydrogen bonds between the fibers and the matrix when the cement absorbs water during wet curing [31–34].

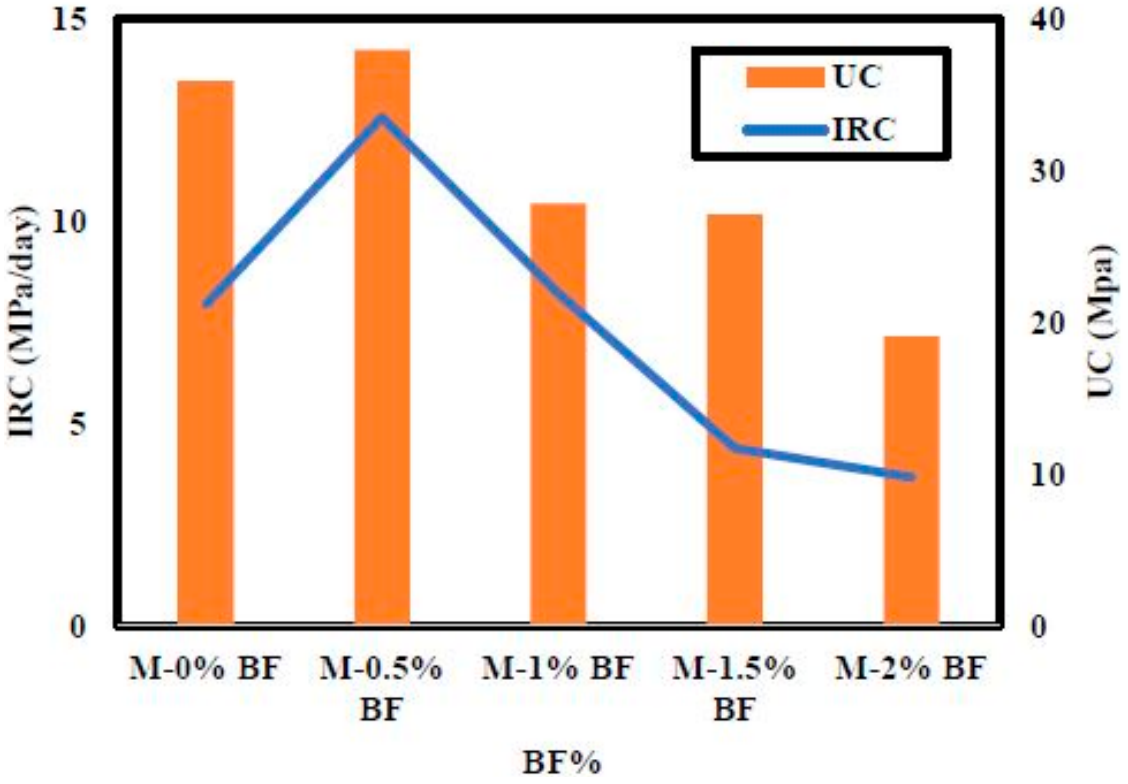

Figure 12. Compressive strength characteristics of mortar with different BF additions.

3.3. Flexural Strength

The flexural strength of different mortar mixes containing BF is shown in Figure 13. At 90 days, the results show that flexural strength was 5.1% higher with the addition of 0.5% BF compared to the control mix. Since BF is naturally resistant to cracking, it delays the beams' failure and improves their capacity to endure stress after peak loading, leading to an increase in the sample's flexural strength [39–42]. Increased fiber content may result in an unequal distribution of fibers inside the matrix, causing clumping. The non-uniform distribution of fibers into the matrix may lead to an ineffective interaction between fibers and mortar at higher fiber contents, leading to bonding issues. This may generate vulnerabilities that undermine the overall integrity of the mortar. Furthermore, the bridging effect produced by BF restricting fracture propagation [40] is responsible for this improvement. Above 0.5% BF addition, in comparison to fiber-free mortar, the flexural strength exhibited a 6.1, 14, and 18.3% drop for M-1% BF, M-1.5% BF, and M-2% BF, respectively, after 90 days. Mixing at 1, 1.5, and 2% BF causes the fibers to wrap and twist, which reduces their effectiveness in stress transfer throughout the total fiber length and, in turn, reduces flexural strength [43,44]. A further potential cause is that the porosity of the mixture is affected by an accumulation of fiber filaments caused by the balling effect [15]. In line with this finding, Lamichhane et al. [18] demonstrated that increasing the BF content increased its flexural strength up to a volumetric fiber content of 0.25%, after which strength began to decrease for higher fiber concentrations. According to another study investigating the fiber-reinforced recycled cement foundation material, the flexural strength of fiber-reinforced recycled-brick-powder cementitious composites increased initially and then declined with the concentration of polyvinyl alcohol (PVA) fiber. Fiber pull-out, fracture, and plastic degradation may be associated with the mechanism of strength drop at high fiber doses [45].

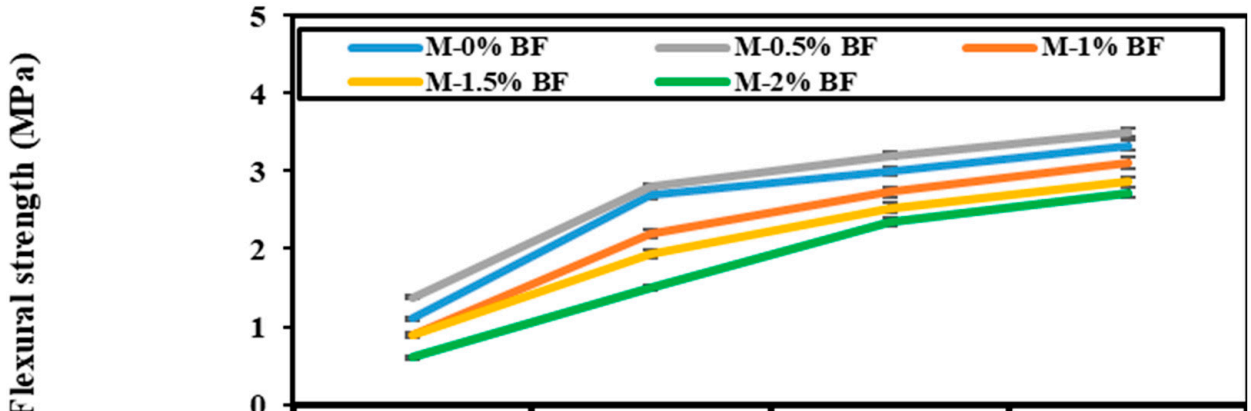

Days	1	7	28	90
M-0% BF	1.10	2.70	3.00	3.33
M-0.5% BF	1.38	2.80	3.20	3.50
M-1% BF	0.90	2.20	2.73	3.10
M-1.5% BF	0.89	1.93	2.53	2.86
M-2% BF	0.60	1.50	2.35	2.72

Figure 13. Flexural strength of mortar with different BF additions.

3.4. Total Water Absorption (TWA)

The TWA results of several mortar mixes containing BF at 1 and 28 days are shown in Figures 14a and 14b, respectively. As shown, there was an increase in TWA from 11.8% for M-0% BF to 15.6% for M-2% BF on day 1 and from 5.1% for M-0% BF to 7% for M-2% BF on day 28. The impact of curing time on the TWA for various mortar mixes is shown in Figure 15a. The % increase in TWA for different mortar mixes compared to the control mix at 1 day and 28 days is displayed in Figure 15b. The results show that as the curing duration increases, TWA drops significantly. For example, the M-1.5% BF TWA decreased from 15.5% at day 1 to 6.2% at day 28. Longer curing durations cause concrete's capillary pores to fill with water, which reduces water absorption over time [46]. Furthermore, it was noted that the TWA is unaffected by the addition of 0.5% BF. Beyond 0.5% BF, the TWA increased gradually with the addition of BF. For example, at 28 days, the TWA percentages for mixes containing 1, 1.5, and 2% BF are 5.7, 6.2 and 7%, respectively. When compared to the control mix, the equivalent increases are 11, 21.8, and 37.1%. This increase may be due to the formation of extra voids within the mortar matrix when the BF concentration surpasses 0.5%. The augmentation of fiber volume causes higher disruption of the matrix's structural integrity, leading to elevated porosity. Thus, the augmented porosity enables faster water penetration, resulting in increased overall water absorption [33,47].

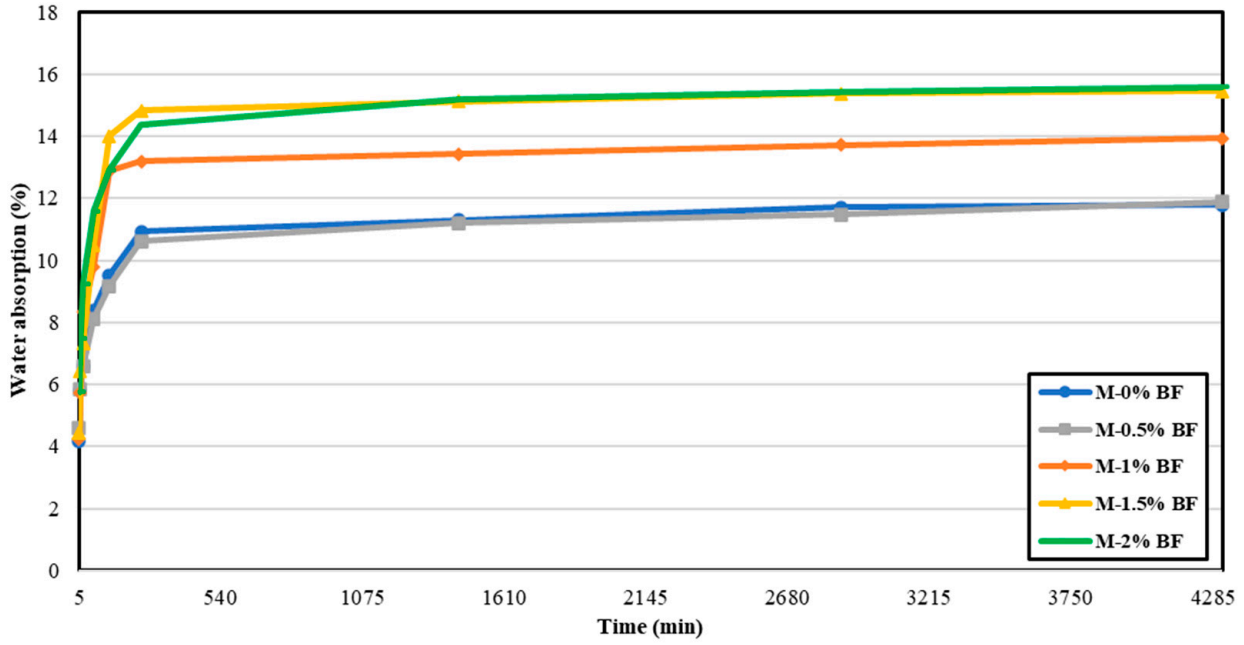

(**a**)

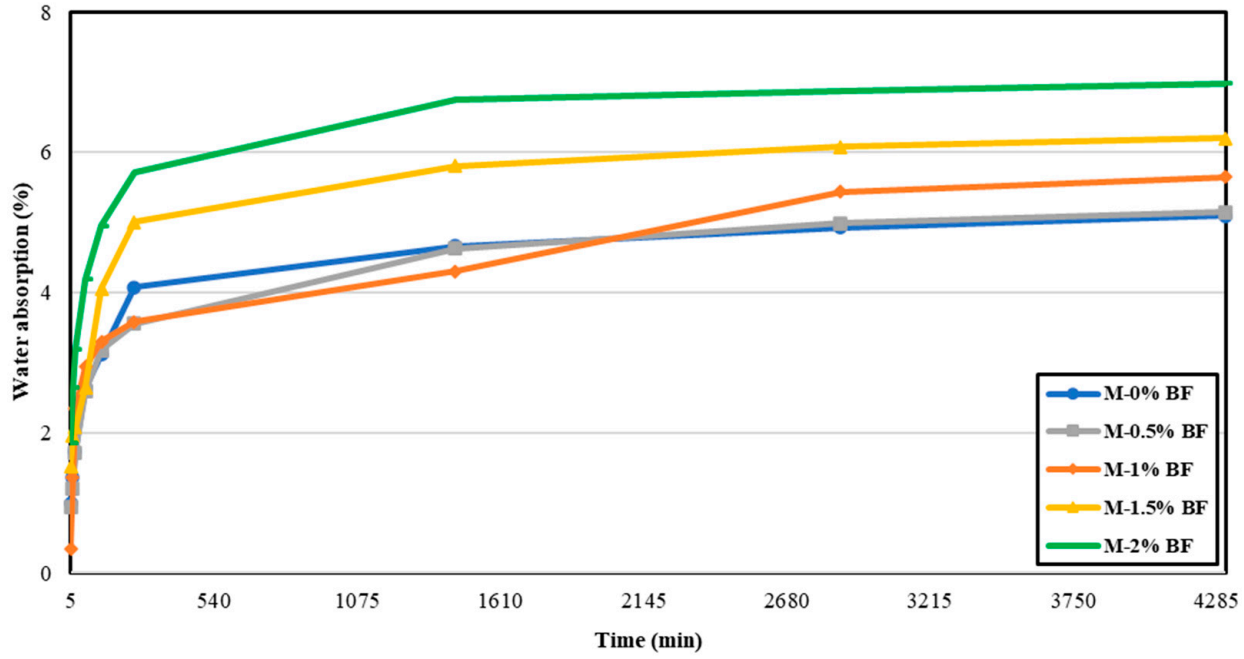

(**b**)

Figure 14. TWA of mortar with different BF additions: (**a**) 1 day; (**b**) 28 days.

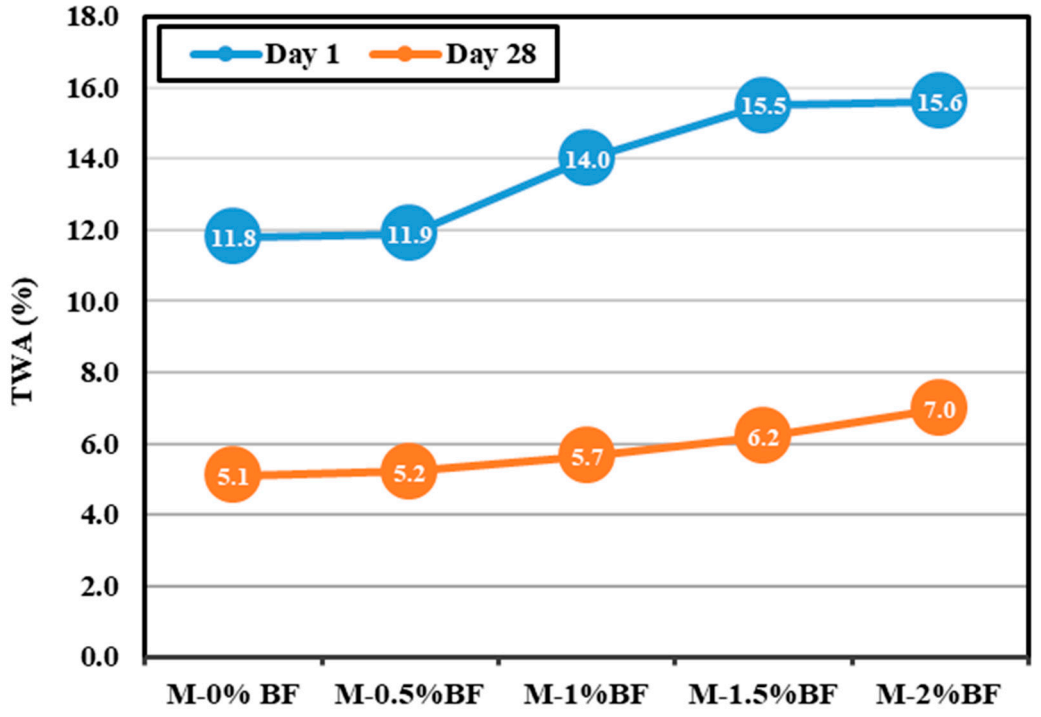

(**a**)

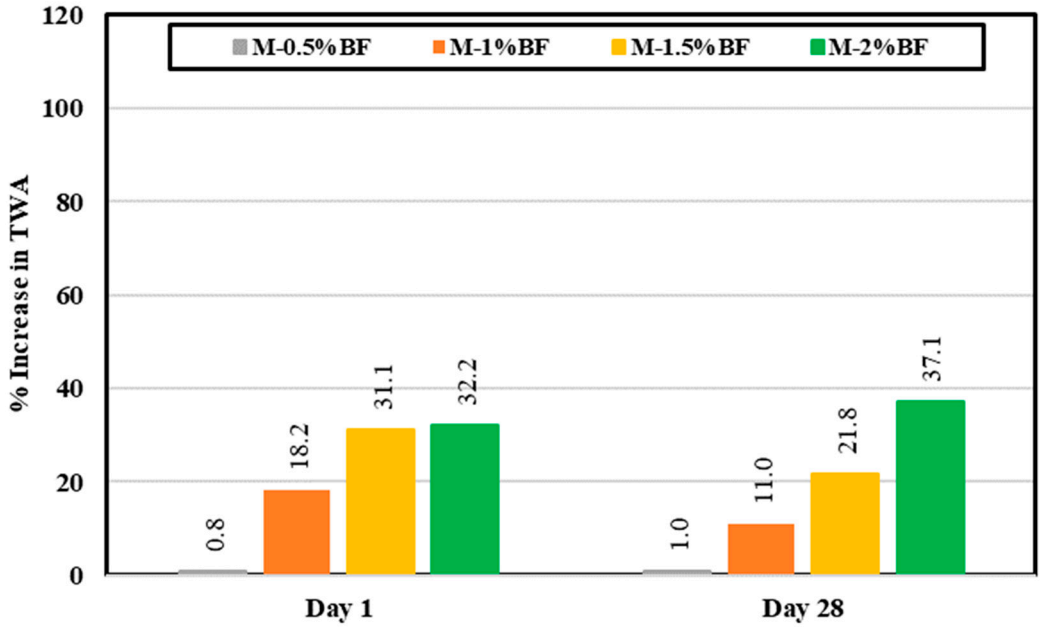

(**b**)

Figure 15. (**a**) Effect of curing duration on TWA coefficients; (**b**) % decrease in TWA at 1 day and 28 days.

3.5. Capillary-Diffusive Process

Figure 16a,b display the weight of absorbed water per area (M/A) results of various mortar mixes incorporating BF at days 1 and 28, respectively. Based on the data, M/A increased from 10 kg/m^2 for M-0% BF to 24.7 kg/m^2 for M-2% BF at day 1, and from 9 kg/m^2 for M-0% BF to 22.65 kg/m^2 for M-2% BF at day 28.

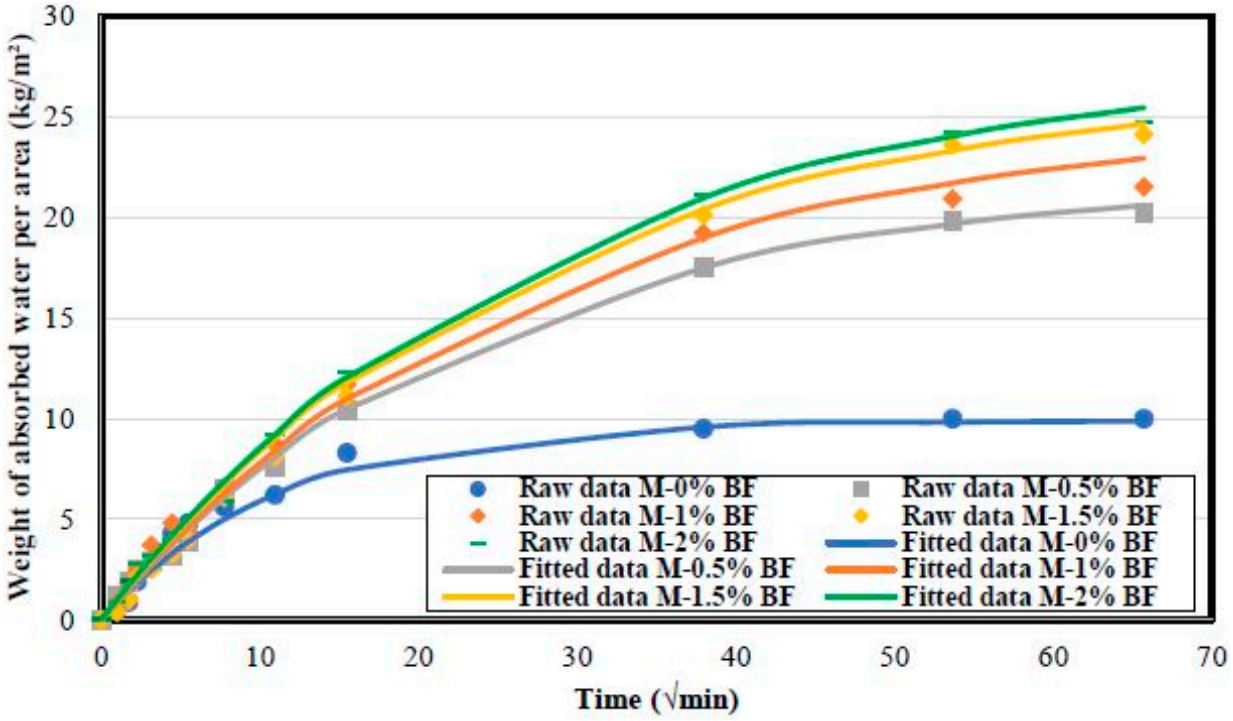

(**a**)

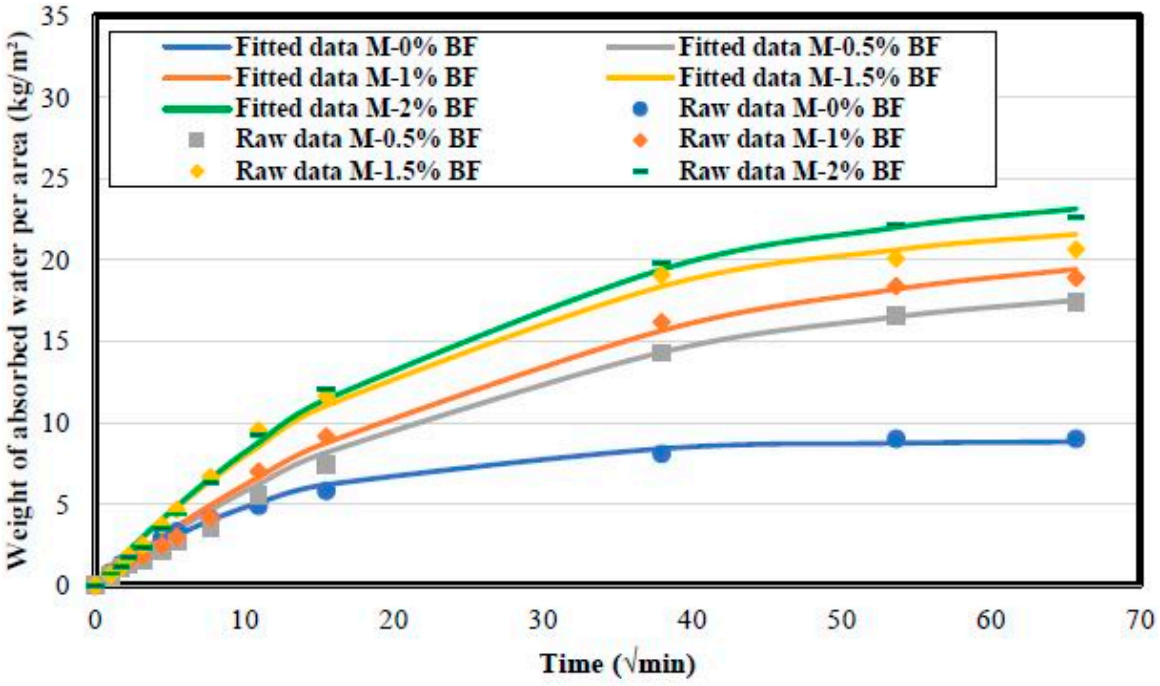

(**b**)

Figure 16. Modeling of capillary-diffusive process of mortar with different BF additions: (**a**) 1 day; (**b**) 28 days.

A capillary-diffusive model was used to estimate the mortars' sorptivity and diffusion coefficients, and the results demonstrated a strong fitting with the experimental data ($R^2 > 0.99$). The values of S, D, and R^2 for all mortar mixes are presented in Table 3.

Table 3. CWA parameters of mortar with different BF additions on days 1 and 28.

Mortar Code	Curing Period (Days)	S ($kg/m^2 \cdot s^{1/2}$)	D (m^2/s)	R^2
M-0% BF	1	1.15×10^{-2}	8.03×10^{-5}	0.983
	28	8.78×10^{-2}	8.05×10^{-8}	0.995
M-0.5% BF	1	1.18×10^{-1}	9.98×10^{-3}	0.997
	28	8.81×10^{-2}	5.61×10^{-7}	0.997
M-1% BF	1	1.20×10^{-1}	5.60×10^{-2}	0.995
	28	9.31×10^{-2}	6.72×10^{-7}	0.996
M-1.5% BF	1	1.29×10^{-1}	7.81×10^{-2}	0.998
	28	1.25×10^{-1}	2.76×10^{-4}	0.995
M-2% BF	1	1.31×10^{-1}	8.24×10^{-2}	0.998
	28	1.27×10^{-1}	2.07×10^{-3}	0.998

As shown, the sorptivity and diffusion coefficients drop significantly as the curing time increases. The sorptivity coefficient of M-1% BF, for example, decreased from 0.115 $kg/m^2 \cdot s^{1/2}$ at day 1 to 0.0878 $kg/m^2 \cdot s^{1/2}$ at day 28. Also, the diffusion coefficient of M-1% BF dropped from 8×10^{-5} m^2/s at day 1 to 8×10^{-8} m^2/s at day 28. The decrease in sorptivity and diffusion coefficients suggests improved performance, as longer curing durations lead to alterations in the internal structure, making it more challenging for water to penetrate through large pores via capillary actions and finer pores via moisture diffusion [46]. Table 3 displays that as the BF% increased, the sorptivity and the diffusion coefficients also rose. For instance, at 28 days, for mixtures containing 0, 0.5, 1, 1.5, and 2% BF, the sorptivity coefficients are 0.0878, 0.0881, 0.0930, 0.1250, and 0.1270 $kg/m^2 \cdot s^{1/2}$, respectively. Because BF is hydrophobic, it will probably absorb adjoining capillary water. As a consequence, capillary forces in the framework will rise. The rise in the sorptivity coefficient is mainly attributed to the supplemented capillary forces arising from the augmented fiber content in the mixtures. Increasing the percentage of BF introduces additional capillary pathways, resulting in enhanced water uptake and greater sorptivity [48].

Regarding the diffusion coefficients, the values are 8.05×10^{-8}, 5.61×10^{-7}, 6.72×10^{-7}, 2.76×10^{-4}, and 2.07×10^{-3} m^2/s for M-0% BF, M-0.5% BF, M-1% BF, M-1.5% BF, and M-2% BF, respectively. The inclusion of BF in mortar can be ascribed to the fibers' capacity to improve the mortar's permeability by building additional pathways for water flow, which results in an increase in diffusion coefficients. The overall diffusion rate is augmented as the proportion of BF increases, as the fiber-induced channels facilitate greater moisture diffusion into the smaller pores of the mortar [48].

3.6. Relationships between Various Properties

3.6.1. Compressive Strength-UPV Relationship

The correlation between compressive strength and UPV is illustrated in Figure 17. The coefficient of determination R^2 values of 0.94, 0.99, 0.98, 0.98, and 0.99 indicate a strong correlation between compressive strength and the UPV for BF percentages of 0, 0.5, 1, 1.5, and 2%, respectively. These findings indicate that an increase in compressive strength will inevitably lead to an increase in the UPV. This significant relationship between the two variables supports the hypothesis that high UPV values represent high-quality mortar with few voids and, consequently, greater compressive strength [46,49].

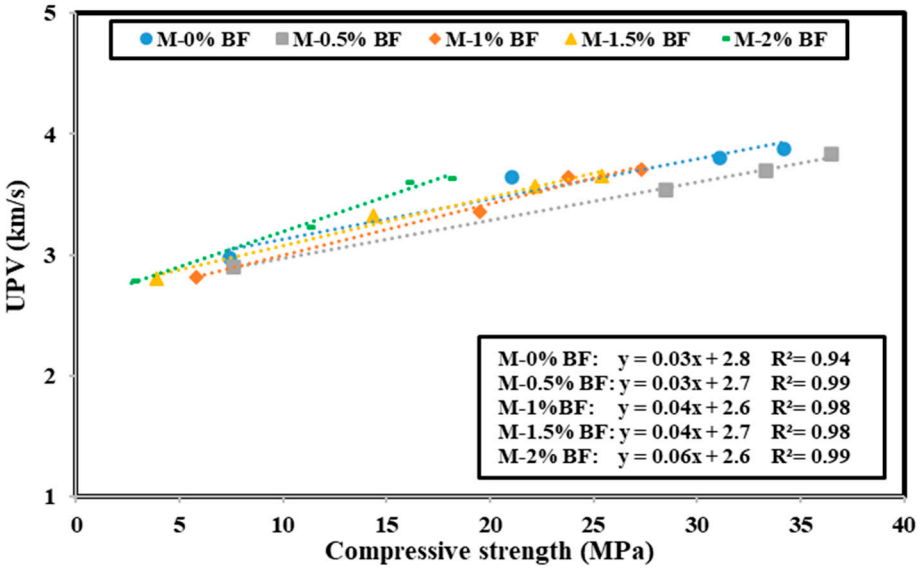

Figure 17. Correlation between compressive strength and UPV.

3.6.2. Compressive Strength–Flexural Strength Relationship

Figure 18 depicts the relationship between compressive strength and flexural strength. For BF percentages of 0, 0.5, 1, 1.5, and 2%, respectively, the coefficient of determination R^2 values of 0.94, 0.99, 0.99, 0.97, and 0.91 demonstrate a strong linear relationship between compressive strength and flexural strength. According to these results, enhancing compressive strength results in increasing flexural strength. As the beams cure, hydration products are formed, which increases the compressive strength of mortar [50]. Similarly, the flexural strength is enhanced due to the beams' enhanced ability to endure stress following peak loading [38].

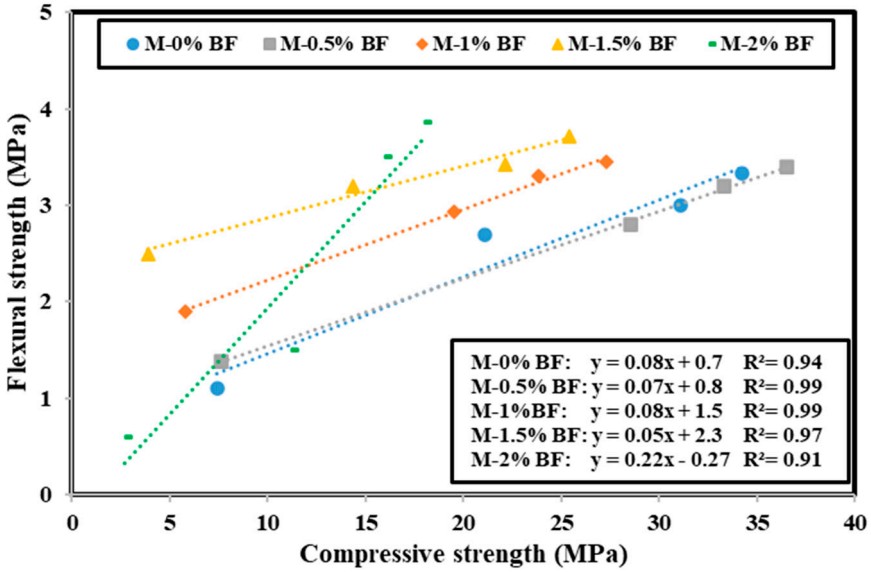

Figure 18. Correlation between compressive strength and flexural strength.

3.6.3. Compressive Strength-(M/A) Relationship

The correlation between compressive strength and M/A is presented in Figure 19. The R^2 values of 0.81, 0.91, 0.84, 0.95, and 0.91 reveal a significant negative relationship between compressive strength and M/A for BF percentages of 0, 0.5, 1, 1.5, and 2%, respectively. These data suggest that an increase in compressive strength will result in a decrease in M/A. As curing days increase, M/A decreases as a result of the augmented density and reduced

permeability of mortar [46]. On the other hand, the gradual formation of hydration products enhances the strength of mortar, which increases the compressive strength over time [50].

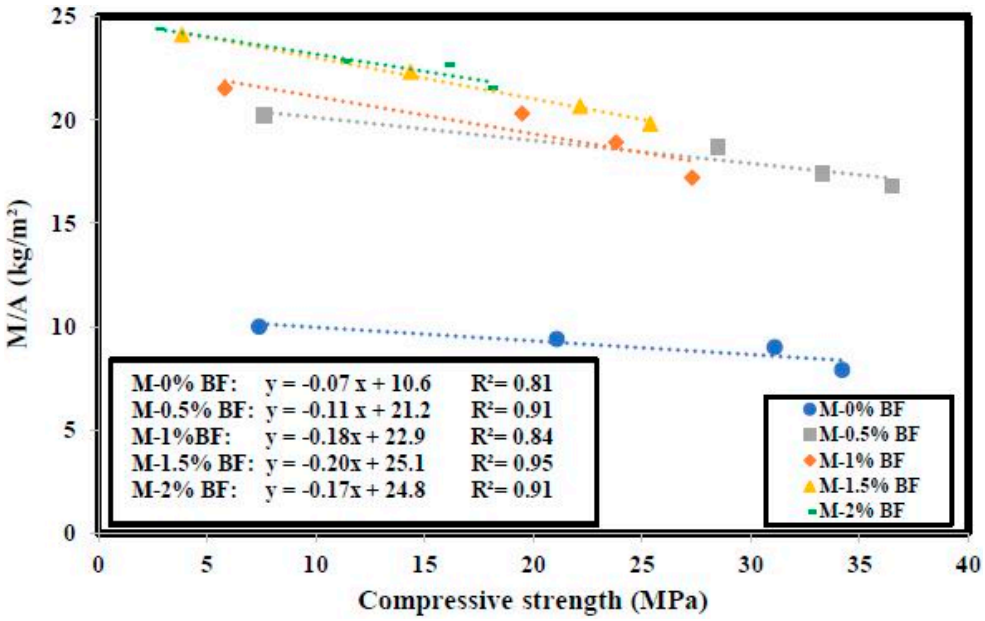

Figure 19. Correlation between compressive strength and M/A.

4. Conclusions

Due to their reduced environmental effect, natural fiber-reinforced cementitious materials offer a practical and long-term substitute for synthetic fiber-reinforced cementitious composites. Banana fiber integration into mortar for pavement applications, including paving blocks, was the focus of the present study. Testing was conducted on the mortar mixtures containing BF to determine their UPV, compressive strength, flexural strength, TWA, sorptivity, and diffusion coefficients. Based on this investigation, the following points can be stated.

- The addition of 0.5% BF resulted in either similar or slightly higher compressive and flexural strength compared to the control. Beyond 0.5%, there is a consistent reduction in mechanical properties.
- A correlation coefficient of $R^2 \sim 0.9$ indicates that the hyperbolic model was effective in predicting the compressive strength over a 90-day period. Both the initial length change and the ultimate length change parameters peaked at 0.5% BF addition and subsequently steadily declined with increasing BF%.
- As the amount of BF added to mortar mixes rises, the TWA increases. With reference to the control, the TWA is increased by 1, 11, 21.8, and 37.1% for mixes containing 0.5%, 1%, 1.5%, and 2% BF, respectively, at 28 days.
- The weight of water absorbed per area increases with the addition of BF to the mortar mixture. M/A is increased by 93, 110, 130, and 152% at 28 days for mixes containing 0.5, 1, 1.5, and 2% BF, respectively, compared to the control mix.
- With a correlation coefficient of $R^2 > 0.99$, the capillary-diffusive model successfully predicted the capillary-diffusive phenomenon as a function of time. The sorptivity and diffusion coefficients exhibited a progressive increase when BF is added and a reduction as the curation period progresses.
- UPV and flexural strength show a strong positive association with compressive strength with high coefficients of correlation ($R^2 \geq 0.9$). On the other hand, M/A is negatively correlated to compressive strength.
- According to this study, BF content of 0.5% in the matrix yields the best mechanical and physical properties, providing appropriate mechanical and durability performance. Future research should consider adding less than 0.5% BF.

Author Contributions: Conceptualization, H.G. and A.E.; Methodology, G.A.-M. and H.G.; Validation, S.E.-Z. and A.E.; Formal analysis, G.A.-M. and H.G.; Writing—original draft, G.A.-M. and H.G.; Writing—review and editing, G.A.-M., J.K., S.E.-Z. and A.E.; Supervision, J.K. and A.E. All authors have read and agreed to the published version of the manuscript.

Funding: This research received no external funding.

Institutional Review Board Statement: Not applicable.

Informed Consent Statement: Not applicable.

Data Availability Statement: Data are contained within the article.

Acknowledgments: The authors express their gratitude for the assistance provided by the staff and technicians at BAU Laboratories.

Conflicts of Interest: The authors declare no conflicts of interest.

References

1. Obi, F.O.; Ugwuishiwu, B.O.; Nwakaire, J.N. Agricultural waste concept, generation, utilization and management. *Niger. J. Technol.* **2016**, *35*, 957–964. [CrossRef]
2. Akinyemi, B.A.; Okonkwo, C.E.; Alhassan, E.A.; Ajiboye, M. Durability and strength properties of particle boards from polystyrene–wood wastes. *J. Mater. Cycles Waste Manag.* **2019**, *21*, 1541–1549. [CrossRef]
3. Tolêdo Filho, R.D.; Ghavami, K.; England, G.L.; Scrivener, K. Development of vegetable fibre–mortar composites of improved durability. *Cem. Concr. Compos.* **2003**, *25*, 185–196. [CrossRef]
4. Al-Massri, G.; Ghanem, H.; Khatib, J.; Kırgız, M.S.; Elkordi, A. Chemical shrinkage, autogenous shrinkage, drying shrinkage, and expansion stability of interfacial transition zone material using alkali-treated banana fiber for concrete. *J. Struct. Integr. Maint.* **2024**, *9*, 2390650. [CrossRef]
5. De Andrade Silva, F.; Mobasher, B.; Toledo Filho, R.D. Cracking mechanisms in durable sisal fiber reinforced cement composites. *Cem. Concr. Compos.* **2009**, *31*, 721–730. [CrossRef]
6. Shah, I.; Li, J.; Yang, S.; Zhang, Y.; Anwar, A. Experimental investigation on the mechanical properties of natural fiber reinforced concrete. *J. Renew. Mater.* **2022**, *10*, 1307. [CrossRef]
7. Khan, M.B.; Shafiq, N.; Waqar, A.; Radu, D.; Cismaș, C.; Imran, M.; Almujibah, H.; Benjeddou, O. Effects of jute fiber on fresh and hardened characteristics of concrete with environmental assessment. *Buildings* **2023**, *13*, 1691. [CrossRef]
8. Prafulla, K.; Nagaraju, A. An experimental study on coir fiber reinforced concrete with ground granulated blast furnace slag and dolomite powder as partial replacement of cement. In *IOP Conference Series: Earth and Environmental Science*; IOP Publishing: Bristol, UK, 2022; Volume 1086, p. 012052. [CrossRef]
9. Machaka, M.; Khatib, J.; Baydoun, S.; Elkordi, A.; Assaad, J.J. The Effect of Adding Phragmites australis Fibers on the Properties of Concrete. *Buildings* **2022**, *12*, 278. [CrossRef]
10. Zouaoui, Y.; Benmahiddine, F.; Yahia, A.; Belarbi, R. Hygrothermal and mechanical behaviors of fiber mortar: Comparative study between palm and hemp fibers. *Energies* **2021**, *14*, 7110. [CrossRef]
11. Li, Q.; Ibrahim, L.; Zhou, W.; Zhang, M.; Yuan, Z. Treatment methods for plant fibers for use as reinforcement in cement-based materials. *Cellulose* **2021**, *28*, 5257–5268. [CrossRef]
12. Mohammed-Ziegler, I.; Oszlánczi, Á.; Somfai, B.; Hórvölgyi, Z.; Pászli, I.; Holmgren, A.; Forsling, W. Surface free energy of natural and surface-modified tropical and European wood species. *J. Adhes. Sci. Technol.* **2004**, *18*, 687–713. [CrossRef]
13. Mohammed-Ziegler, I.; Tánczos, I.; Hórvölgyi, Z.; Agoston, B. Water-repellent acylated and silylated wood samples and their surface analytical characterization. *Colloids Surf. A Physicochem. Eng. Asp.* **2008**, *319*, 204–212. [CrossRef]
14. Arias, P. The World Banana Economy 2003, 1985–2002 (No. 1). Food & Agriculture Org. Available online: https://www.fao.org/3/y5102e/y5102e04.htm (accessed on 15 September 2024).
15. Ali, B.; Azab, M.; Ahmed, H.; Kurda, R.; El Ouni, M.H.; Elhag, A.B. Investigation of physical, strength, and ductility characteristics of concrete reinforced with banana (Musaceae) stem fiber. *J. Build. Eng.* **2022**, *61*, 105024. [CrossRef]
16. Logeshwar, A.B.; Bhuvaneshpandi, M.; Harishkanna, V.; Midhunkumar, R.; Praveenkumar, S. Effect of Banana Fibre on Strength Properties of Bagasse ash & Rice Husk ash blended high performance concrete composite. In Proceedings of the ASPS Conference Proceedings, Rajasthan, India, 19–22 December 2022; Volume 1, pp. 201–206. [CrossRef]
17. Pathan, T.A.; Jhumarwala, R.A. Evaluation of mechanical properties of high strength banana fibre concrete (HSBFC) incorporating fly ash and silica fume. *Int. J. Res. Appl. Sci. Eng. Technol.* **2022**, *10*, 780–785. [CrossRef]
18. Lamichhane, N.; Lamichhane, A.; Gyawali, T.R. Enhancing mechanical properties of mortar with short and thin banana fibers: A sustainable alternative to synthetic fibers. *Heliyon* **2024**, *10*, e30652. [CrossRef]
19. Thanushan, K.; Sathiparan, N. Mechanical performance and durability of banana fibre and coconut coir reinforced cement stabilized soil blocks. *Materialia* **2022**, *21*, 101309. [CrossRef]

20. *ASTM C1437-15 2015*; Standard Test Method for Flow of Hydraulic Cement Mortar. ASTM International: West Conshohocken, PA, USA, 2015.
21. *ASTM C 597*; Standard Test Method for Pulse Velocity through Concrete. American Society for Testing and Materials: West Conshohocken, PA, USA, 2016.
22. Ghanem, H.; Khatib, J.; Elkordi, A. Effect of partial replacement of sand by mswi-ba on the properties of mortar. *BAU J. Sci. Technol.* **2020**, *1*, 4. [CrossRef]
23. *ASTM C109*; Standard Test Method for Compressive Strength of Hydraulic Cement Mortars (Using 2-in. or [50 mm] Cube Specimens. ASTM International: West Conshohocken, PA, USA, 2016.
24. Ghanem, H.; Ramadan, R.; Khatib, J.; Elkordi, A. A Review on Chemical and Autogenous Shrinkage of Cementitious Systems. *Materials* **2024**, *17*, 283. [CrossRef]
25. *ASTM C348*; Standard Test Method for Flexural Strength of Hydraulic-Cement Mortars. American Society for Testing and Materials International: West Conshohocken, PA, USA, 2008.
26. *ASTM C1585*; Standard Test Method for Measurement of Rate of Absorption of Water by Hydraulic-Cement Concretes. ASTM International: West Conshohocken, PA, USA, 2004.
27. Martys, N.S.; Ferraris, C.F. Capillary transport in mortars and concrete. *Cem. Concr. Res.* **1997**, *27*, 747–760. [CrossRef]
28. Villar-Cocina, E.; Valencia-Morales, E.; Vega-Leyva, J.; Munoz, J.A. Kinetics of the water absorption in GGBS-concretes: A capillary-diffusive model. *Comput. Concr. Int. J.* **2005**, *2*, 19–30. [CrossRef]
29. Wongsa, A.; Kunthawatwong, R.; Naenudon, S.; Sata, V.; Chindaprasirt, P. Natural fiber reinforced high calcium fly ash geopolymer mortar. *Constr. Build. Mater.* **2020**, *241*, 118143. [CrossRef]
30. Mathavan, M.; Sakthieswaran, N.; Babu, O.G. Experimental investigation on strength and properties of natural fibre reinforced cement. *Mater. Today Proc.* **2021**, *37*, 1066–1070. [CrossRef]
31. Alatshan, F.; Altlomate, A.M.; Mashiri, F.; Alamin, W. Effect of date palm fibers on the mechanical properties of concrete. *Int. J. Sustain. Build. Technol. Urban Dev.* **2017**, *8*, 68–80. [CrossRef]
32. Khatib, J.M.; Ramadan, R.; Ghanem, H.; Elkordi, A.; Baalbaki, O.; Kırgız, M. Chemical shrinkage of paste and mortar containing limestone fines. *Mater. Today Proc.* **2022**, *61*, 530–536. [CrossRef]
33. De La Grée, G.D.; Yu, Q.L.; Brouwers, H.J.H. Assessing the effect of $CaSO_4$ content on the hydration kinetics, microstructure and mechanical properties of cements containing sugars. *Constr. Build. Mater.* **2017**, *143*, 48–60. [CrossRef]
34. Bilba, K.; Arsène, M.A.; Ouensanga, A. Sugar cane bagasse fibre reinforced cement composites. Part I. Influence of the botanical components of bagasse on the setting of bagasse/cement composite. *Cem. Concr. Compos.* **2003**, *25*, 91–96. [CrossRef]
35. Tolêdo Filho, R.D.; Scrivener, K.; England, G.L.; Ghavami, K. Durability of alkali-sensitive sisal and coconut fibres in cement mortar composites. *Cem. Concr. Compos.* **2000**, *22*, 127–143. [CrossRef]
36. Araya-Letelier, G.; Antico, F.C.; Carrasco, M.; Rojas, P.; García-Herrera, C.M. Effectiveness of new natural fibers on damage-mechanical performance of mortar. *Constr. Build. Mater.* **2017**, *152*, 672–682. [CrossRef]
37. Choi, J.I.; Jang, S.Y.; Kwon, S.J.; Lee, B.Y. Tensile behavior and cracking pattern of an ultra-high-performance mortar reinforced by polyethylene fiber. *Adv. Mater. Sci. Eng.* **2017**, *2017*, 5383982. [CrossRef]
38. Aslon MW, B.; Lakawa, I.; Sulaiman, S.; Hawa, S. Testing the Compressive Strength of Concrete With the Utilization of Rice Husk Ash and Palm Fiber. *Sultra Civ. Eng. J.* **2023**, *4*, 11–19. [CrossRef]
39. Wang, Y.; Cheng, J.; Wang, J. Flexural performance of recycled concrete beam reinforced with modified basalt fiber and nano-silica. *Case Stud. Constr. Mater.* **2023**, *18*, e02022. [CrossRef]
40. Hannawi, K.; Bian, H.; Prince-Agbodjan, W.; Raghavan, B. Effect of different types of fibers on the microstructure and the mechanical behavior of ultra-high performance fiber-reinforced concretes. *Compos. Part B Eng.* **2016**, *86*, 214–220. [CrossRef]
41. Arshad, S.; Sharif, M.B.; Irfan-ul-Hassan, M.; Khan, M.; Zhang, J.L. Efficiency of supplementary cementitious materials and natural fiber on mechanical performance of concrete. *Arab. J. Sci. Eng.* **2020**, *45*, 8577–8589. [CrossRef]
42. Mounanga, P.; Khelidj, A.; Loukili, A.; Baroghel-Bouny, V. Predicting $Ca(OH)_2$ content and chemical shrinkage of hydrating cement pastes using analytical approach. *Cem. Concr. Res.* **2004**, *34*, 255–265. [CrossRef]
43. Kouta, N.; Saliba, J.; Saiyouri, N. Effect of flax fibers on early age shrinkage and cracking of earth concrete. *Constr. Build. Mater.* **2020**, *254*, 119315. [CrossRef]
44. Alzebdeh, K.I.; Nassar, M.M.; Arunachalam, R. Effect of fabrication parameters on strength of natural fiber polypropylene composites: Statistical assessment. *Measurement* **2019**, *146*, 195–207. [CrossRef]
45. Ji, Y.; Ji, W.; Zhang, Z.; Wang, R. Road performance investigation on fiber-reinforced recycled cement base material. *Polymers* **2022**, *14*, 4102. [CrossRef]
46. Ghanem, H.; Machaka, M.; Khatib, J.; Elkordi, A.; Baalbaki, O. Effect of partial replacement of cement by MSWIBA on the properties of mortar. *Acad. J. Civ. Eng.* **2019**, *37*, 82–89. [CrossRef]
47. Khatib, J.; Ramadan, R.; Ghanem, H.; ElKordi, A. Effect of using limestone fines on the chemical shrinkage of pastes and mortars. *Environ. Sci. Pollut. Res.* **2023**, *30*, 25287–25298. [CrossRef]
48. Ren, F.; Zhou, C.; Zeng, Q.; Ding, Z.; Xing, F.; Wang, W. The dependence of capillary sorptivity and gas permeability on initial water content for unsaturated cement mortars. *Cem. Concr. Compos.* **2019**, *104*, 103356. [CrossRef]

49. Khatib, J.; Ramadan, R.; Ghanem, H.; Elkordi, A. Volume stability of cement paste containing limestone fines. *Buildings* **2021**, *11*, 366. [CrossRef]
50. Pipilikaki, P.; Katsioti, M. Study of the hydration process of quaternary blended cements and durability of the produced mortars and concretes. *Constr. Build. Mater.* **2009**, *23*, 2246–2250. [CrossRef]